



Rehabilitation of Portal Subsidence of Heybat Sultan Twin Tunnels: Selection of Shotcrete or Geogrid Alternatives

Ako Daraei¹ · Bengin M. Herki¹ · Aryan Far H. Sherwani¹ · Shokrollah Zare²

Received: 10 April 2018 / Accepted: 18 April 2018 / Published online: 26 April 2018
© Springer International Publishing AG, part of Springer Nature 2018

Abstract

The occurrence of karst phenomenon is one of the common problems in carbonate rocks in the presence of water. The rock masses constituting the ground surface are mostly of sedimentary types among which carbonate rocks are widely observed. It is therefore necessary to accept such a geological hazard in many projects. Some of the rehabilitation methods for karstic subsidence include grout injection, filling with concrete or shotcrete and making use of geosynthetic products. Few studies have been carried out on the application of the geosynthetic products. Limy rocks form the main lithology of a large part of the 72 km long access road tunnel designed for the Iraqi-Kurdistan. The occurrence of a karstic subsidence with a volume of about 2250 m³ in the portal of Heybat Sultan tunnels revealed the necessity of examining and selecting one of these rehabilitation methods. Concerns about the repetition of such collapses in other tunnels, especially in the 6740 m long Korek twin tunnels that is the longest tunnel of the Middle East located in the vicinity of the project, has doubled the importance of the issue. This paper aims to render an account of the use of shotcrete and geogrid to rehabilitate the subsidence of the portal of Heybat Sultan tunnels. The modeling results with the FLAC numerical finite difference code showed that the displacement amount of the host rock mass after implementing the second method would be 2.9 times less than the first method. Geogrid also reduces the axial forces exerted to the tunnel supporting system up to 43 tons.

Keywords Subsidence · Karst · Geogrid · Shotcrete · Tunneling

Introduction

The phenomenon of erosion and dissolution of carbonate rock masses, such as limestone, gypsum and dolomite, is called karst. This phenomenon also occurs in other dissolved rocks such as sulfate and chloride rocks. Due to higher solubility and lower mechanical strength, sinkholes (dolines) usually have a higher probability of occurrence and a greater genetic diversity in evaporate terrains rather than in carbonate karst areas. The generation of karstic depressions is related to the dissolution of carbonate and evaporative rocks [1]. The formation of karst depends on two factors: (1) the rock mass has the potential of

dissolving; (2) Everything is prepared to form a groundwater system. It is necessary to make use of the geological maps, aerial photographs, surface mappings, rainfall measurements of the region and geophysical methods to identify the potential Karst zones. Due to the exposure to the karst lands, major studies in the field of recognition and rehabilitation methods have been carried out by Chinese researchers. Li et al. [2] reported that about one-third of the area of China was covered by Karst. Dealing with karst conditions during the tunnel construction is accompanied by serious risk of water inrush and mortal and financial losses subsequently. In many projects with karst areas identified during the preliminary studies, the alternative of the reject can be the best choice, because the engineering experiences have shown that the rehabilitation of such projects is time consuming, costly, and need to be monitored on regular basis. The rehabilitation of karstic collapses in tunneling projects in recent decades has attracted many researchers including Cui et al. [3], Alija et al. [4], Song et al. [5], Li et al. [6], Huang et al. [7] and Li et al. [2].

✉ Ako Daraei
Daraii2004@yahoo.com

¹ Civil Engineering Department, Soran University, Soran, Kurdistan, Iraq

² School of Mining, Petroleum & Geophysics Engineering, Shahrood University of Technology, Shahrood, Iran

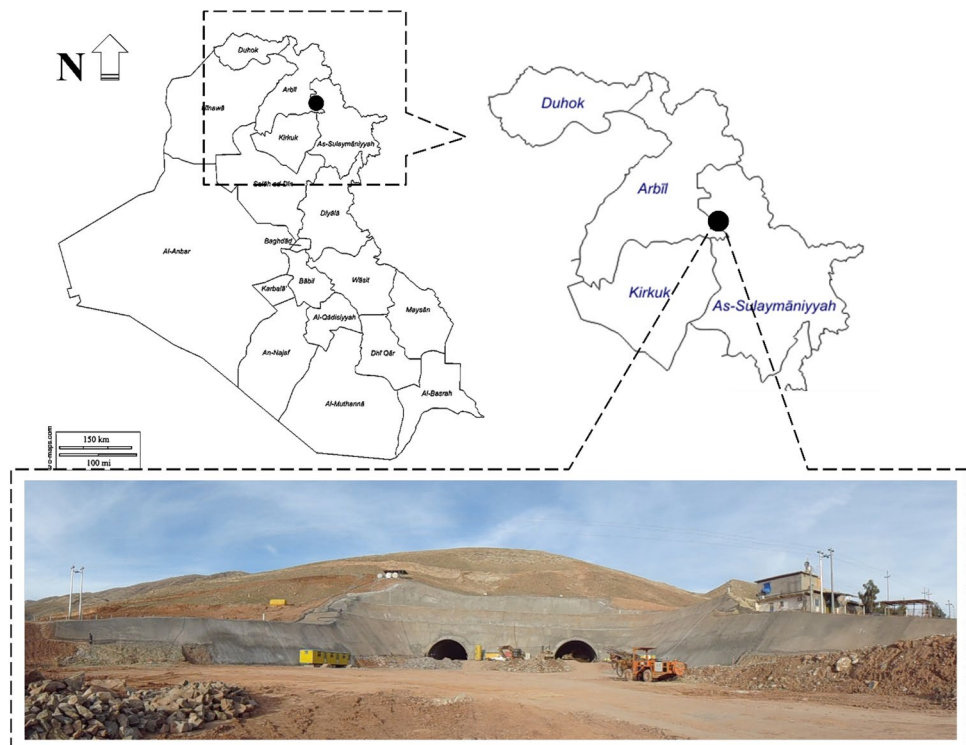
Despite the diversity of geosynthetic products since the early 1980s, the main rehabilitation methods utilized in the karstic cavities and their associated subsidence are still to inject grout and fill them with concrete and shotcrete. Nevertheless, the injection of grout into fractured rock masses due to numerous jointing, the complexity of the joints network and the uncertainties involved will require a great deal of time and cost. Application of geosynthetics is a well-known technique in geotechnical engineering. The main functions of them consist of separation, filtration, drainage, and reinforcement [8]. Geogrid reinforcement is known to be an effective method to enhance the performance and service life of different earth structures [9]. Geogrids have more and more successfully been used in recent times for the construction of steep slopes and geogrid reinforced bridge abutments. This material shows significant advantages in terms of economic and ecological aspects against classical concrete structures [10]. Many studies have been performed on geogrid [8–21], but most of them are either on a laboratory scale or have been done in the pavements and buildings foundation. Besides, less attention has been given to the rehabilitation of collapses in large slopes, especially based on practical cases. Ziegler [10], Liu et al. [22], Ali [23] can be taken into consideration amongst the limited studies performed on this category. The development plan for the infrastructures of Iraqi Kurdistan has begun since 2007. In the designed master plan, the highways of this area have 72 km of tunnels and > 10 km of bridges. Due to the presence of problematic

soils and dissolution rocks, swelling, landslide and karst are observed in many regions of Iraqi Kurdistan [24]. Collapses and observation of karst cavities in a number of tunnels constructed and under construction, such as Sork and Heybat Sultan, on the one hand, and the host rock mass of limestone in a large part of the designed projects on the other hand, have grown concerns about repetition of such hazards in other projects. The presence of troublesome soils in the region, as well as the largest tunnel in the Middle East, Korek twin tunnels with a length of 6740 m and a maximum overburden of 1100 m in limestone rocks in the foregoing master plan reveals the importance of studying on this matter more than before. In this paper, the rehabilitation of the karst subsidence of Heybat Sultan tunnels portal is investigated using two alternatives of geogrid and shotcrete.

Project Specifications

Twin tunnels of Heybat Sultan are being constructed as part of the Erbil-Sulaymaniyah highway at 5 km from the Koya. The tunnels with a length of 2×2600 m, 110 m^2 cross section, and a minimum and maximum tunnel overburden of 9 and 296 m are located in the northeast of Iraq in Kurdistan region as shown in Fig. 1. The construction of this project will eliminate the arduous defile of Heybat Sultan so that the road accidents will significantly be reduced.

Fig. 1 The close up view of Heybat Sultan twin tunnels



Geological and Rock Mechanical Properties

This area is geologically composed of pre-Quaternary sediments. Outcropped formations belong to the Cretaceous, Paleocene and Neocene periods, and Miocene epoch to Upper Cretaceous [25]. The most recent outcrops are observed at the portal of the tunnels, and as the age of the geological units of the area increases towards the tunnel outlet. The lithology of the host rock mass of the tunnels consists mainly of limestone, gypsum, marlstone, shale and claystone. The study area, as part of the Zagros high folded zone [26], has been subject to a lot of structural deformities. The folds existing in the study area are of anticline type with strike of mainly NW–SE. Such a situation, in addition to fracturing the host rock masses, also has had intensive changes in the thickness of the layers at short distances (Fig. 2).

Based on the geomechanical characteristics of the rocks, the tunnels area was divided into six blocks (Fig. 3). In terms of geomechanical classification [27], the rock masses are classified as very poor to poor (IV, V). This factor, along with the large area of the tunnel section, is one of the main reasons for choosing the top heading and benching method for excavation. The tunnel supporting system in the weakest rock mass class, including the I-160@0.5 m steel ribs embedded in 25 cm of shotcrete together with 6 m long and 28 mm diameter rock bolts

with 1 × 1 m pattern as shown in Fig. 4a. In order to control the tunnel deformations and transfer the loads exerted on the supporting system to both sides, elephant foot technique was applied at the head and bench connection point in accordance with Fig. 4b.

Since the in-situ tests are so costly, the geomechanical properties of the rock masses existing along the tunnels route are determined using the results of laboratory tests conducted on the intact rock samples obtained from the boreholes drilled in the longitudinal axis of the tunnel; then, the rock mass parameters are obtained using the Roc-Data code according to Table 1.

153 joints were mapped by implementing scan line from 7 outcrops along the tunnels route. The joints in filling is mainly clayey, the joints surface is smooth to slightly rough, and the weathering in the joints surfaces is moderate to high. Four sets of discontinuities were identified in this area (Table 2) after drawing the joints in the Dips code as shown in Fig. 5a. Such an environment in the geomechanical literature will be classified as crushed class and pseudo-continua.

Rose diagrams, also called polar bar plots, are useful for showing azimuthal (directional) data. Any dataset consisting of lots of measurements of direction or orientation could visualize this way. By drawing the rose diagram of the joints, as shown in Fig. 5b, the general trend of the joints was determined as NE–SW. With regard to the

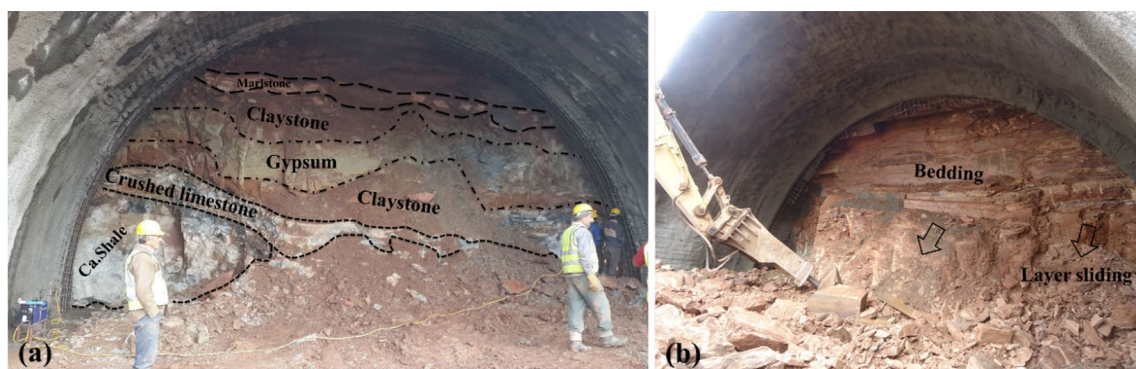


Fig. 2 a Folding and change in the thickness of the layers, b slide of the layers inside the tunnel

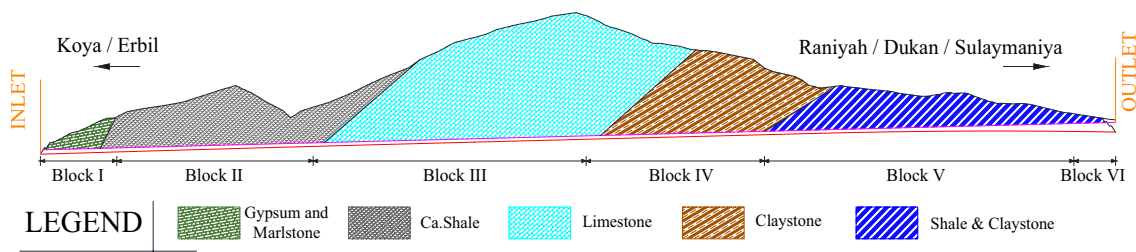


Fig. 3 Longitudinal section

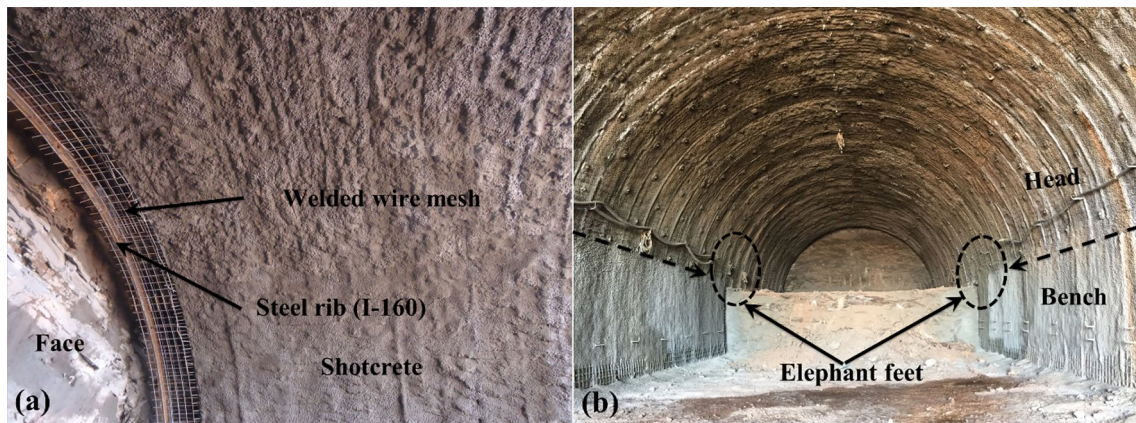


Fig. 4 a Supporting system, b applying elephant foot technique at the head and bench connection point

Table 1 Rock mass properties

Block	Lithology	c (kPa)	φ (°)	E_m (MPa)	GSI	RMR	Q
I	Gypsum, marly limestone and siltstone	39	43	740	22	27	0.14
II	Marlstone	213	31	1521	30	25	0.12
III	Limestone	514	32	5236	42	37	1.03
IV	Claystone	325	31	2162	38	33	0.15
V	Shale and claystone	104	19	769	28	23	0.02
VI	Claystone	80	22	786	28	23	0.02

Table 2 Joint sets properties in the tunnel path

Discontinuity set	Average dip/dip direction	Average spacing (cm)	Average persistence (m)
Js-A	20/120	40–80	1–3
Js-B	42/210	30–60	3–8
Js-C	12/305	1–2	> 10
Js-D	45/045	50–90	2–4

azimuth of the tunnels (50°), it can be concluded that the discontinuities are mainly parallel to the tunnels direction. This is one of the main reasons for the slide of layers into the tunnel during the excavation (Fig. 2b).

Inlet Portal Collapse

In March 2015, after a successive precipitations, a collapse with dimensions of $30 \times 15 \times 15$ m occurred in the tunnels inlet portal as shown in Fig. 6a. The inlet portal was implemented in three benches with heights of 7, 8 and 15 m, slope of 1:1 (45°) and berms width of 5 m. the tunnel supporting system is implemented as a 15 cm thick shotcrete

layer reinforced with a $Q221/221$ ($\phi 6.5 @ 150 \times 150$) layer of wire mesh, drilling of 3 and 6 m long drainage holes with the arrangement of 4×6 and 3.5×3.5 m, and the installation of a 6 m long and 28 mm diameter pre-bolts around and on the wall between the tunnels. The ease of entering the surface runoffs into the portal and the presence of dissolving gypsum rock mass (Fig. 6b) can be the most important reasons for collapsing [28]. Although the effect of water on critical and failure strains is negligible, it will strongly affect the rock strength [29]. Studies show that both the solution and erosion processes have occurred in the karsts zones.

During the geological mapping, some cavities caused by the dissolution of gypsum rocks were observed at chainage 0 + 620 at a distance of 220 m from the tunnel inlet, as shown in Fig. 7. Studies depicted that the depth of these cavities ranges between 10 and 20 m and have a diameter of about 1.5 m. The presence of such cavities in the face grew worries about the tunnel water inrush. In terms of the failure modes, water inrush has been divided into three patterns; geological defects inrush, non-geological defects and combinations of the above two forms [2].

In order to rehabilitate the portal subsidence, three methods of (1) the use of light concrete and injection of

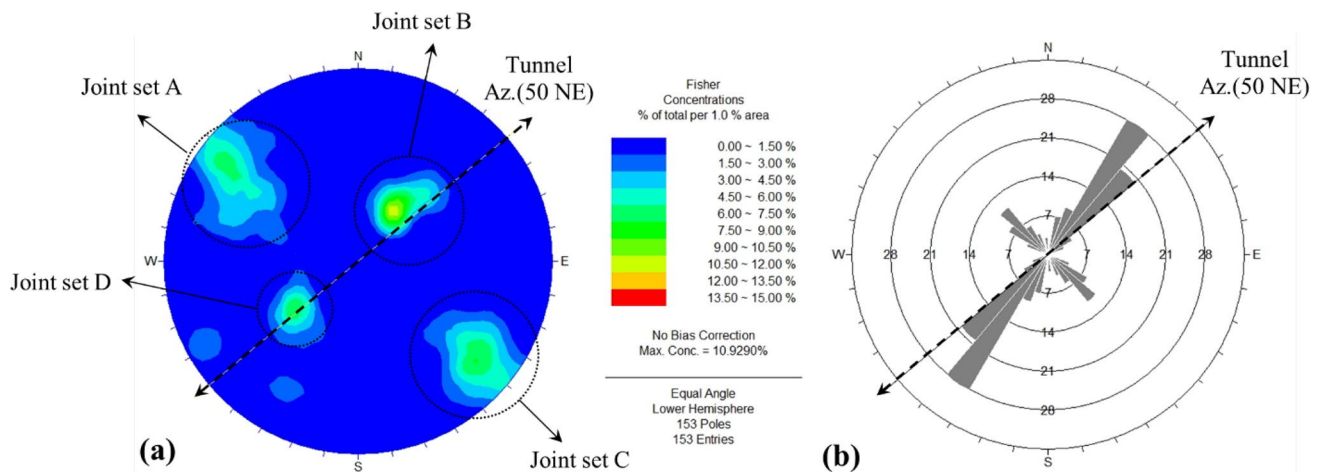


Fig. 5 a Plot of discontinuities, b rose diagram

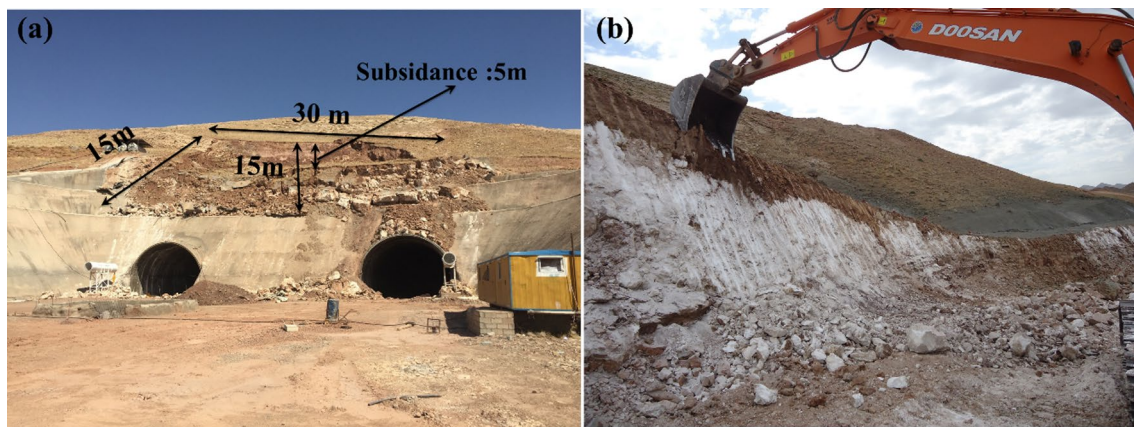


Fig. 6 a Collapse of Heybat Sultan portal, b outcrop of the gypsum layer at first berm of the inlet portal

cement grout (2) the application of shotcrete and (3) the technique of reinforced soil with geogrid were proposed. The first alternative was rejected due to the negative effects of cement grout on groundwater and the high volume of grout consumption due to the crushed rock mass existing in the study area. Numerical analysis will be performed to select one of the second and third alternatives. In general, the method that satisfies the two conditions of minimum displacement in the portal and the minimum forces exerted to the tunnel supporting system will be selected. In the case of using the shotcrete, styrofoam will first be used as filler in deep sections. Styrofoam reduces the shotcrete volume and gives rise to less dead load to be applied to the tunnel supporting system. The method statement of the reinforced soil technique is to implement geogrid layers at certain intervals and to fill the intervals between them with well graded sand. The spacing between the geogrid layers is one of the most influential items in

the mechanical strength of reinforced soils [8]. Sensitivity analysis has been used to determine the spacing. The results showed that if the geogrid is installed at intervals of 3 m, the critical shear strain in the portal will be less than the other cases. Generally, sandy soils are preferred as the backfill soil/neighborly soil for geosynthetics in reinforced soil structures [30], because it would highly affect the drainage of surface water and reducing pore pressure in the study area.

Numerical Modeling

Due to the high fracturing of the host rock mass, its mechanical behavior is categorized as pseudo-continua. For this purpose, the code of finite difference of FLAC [31] was selected. This code is highly able to simulate the large strain modes as well as the soil-structure interaction behaviors. The dimensions of the model are 153×80 m (Fig. 8)

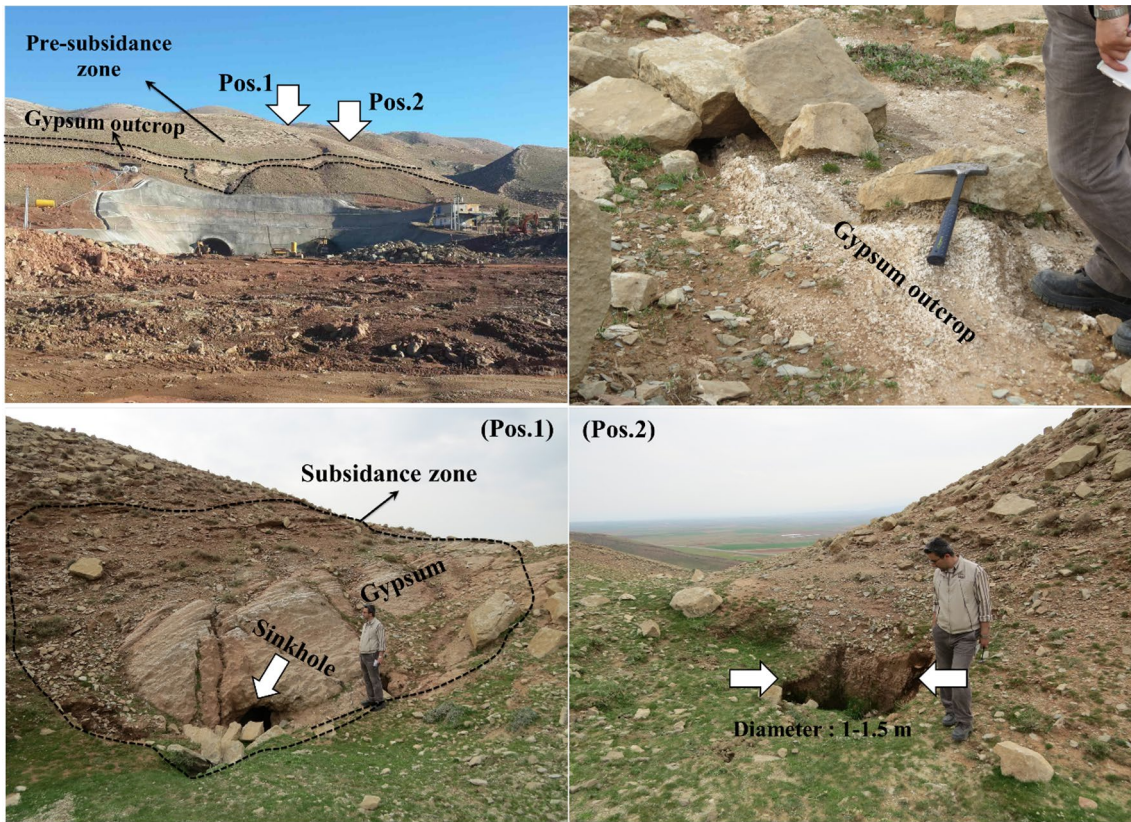


Fig. 7 Karstic cavities in the tunnel excavation route

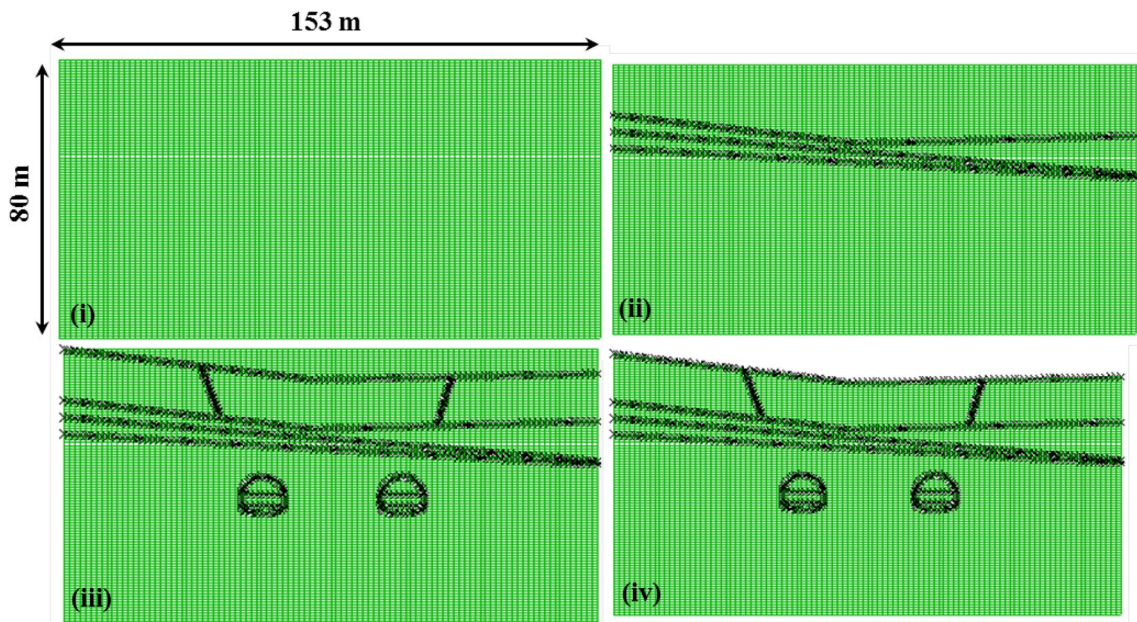


Fig. 8 Model dimensions and procedure of simulations

and the Mohr–Coulomb failure criterion was used to simulate the constitutive model. The vertical stress acting on the rock mass in which these tunnels will be excavated is given by the product of the depth below surface and the unit weight of the rock. Horizontal stress magnitudes and directions can vary greatly, depending upon the tectonic history of the area, the variation in stiffness of different rock units in the rock mass and the local topography [32]. As a starting point for this analysis it has been assumed that the ratio of vertical to horizontal stresses in out of plane is 2 and in-plane is 1.5.

Simulation is done in nine steps: create initial stresses, balance the model, excavate the tunnels heading, primary supporting system installation, checking the stability of the supporting system, cause collapse in the portal, rebalance, fill the collapsed space of the portal, and displacement control. Beam element was used for modeling the steel rib and shotcrete, and cable element was used for the geogrid. Beam elements may be used to model a wide variety of supports, including support struts in an open-cut excavation and concrete or shotcrete linings in a tunnel. Cable elements are used to model a wide variety of supports for which tensile capacity is important, including rock bolts, cable bolts and tiebacks. The definition of interface elements and related parameters for the proper expression of soil-structure interactions is the most important point in geogrid modeling. The most important parameters, in this regard, are the normal and

shear stiffness, cohesion and the friction angle between the surfaces. The cable is connected to the soil grid via interface elements attached on both sides. The interface nodes are assigned low shear strength (approximately 2/3 of the soil friction angle) to simulate a relatively smooth geogrid-to-soil interface. Pullout resistance and interface friction resistance of the geogrids are crucial design [11]. Different parameters for simulating the proposed methods have been taken into consideration as Table 3. It should be noted that the cohesion and internal friction angle of shotcrete will vary considerably depending on temperature conditions, mixing design, type of accelerator and material quality [33].

After generating the model, it is necessary to control the maximum unbalanced nodal forces and node velocity for controlling the equilibrium and accuracy of the model according to Fig. 9 in the FLAC code. In the case that both graphs tend to zero, the model is in equilibrium, otherwise plastic failure would occur in the model.

Discussion

Based on Fig. 10, the vertical and horizontal displacement along AB line of the collapsed zone show that the maximum vertical and horizontal displacement values are 37.5 and 6.76 mm in case of using shotcrete and the maximum vertical and horizontal displacement values are 12.96 and

Table 3 Properties of various materials in numerical modeling

Materials	Density (g/cm ³)	<i>c</i> (kPa)	ϕ (°)	<i>E</i> (MPa)	Yield (MPa)	Area (m ²)	<i>K_b</i> (N/m/m)	<i>S_b</i> (N/m)	Tensile strength (kN/m)
Sand	1.8	0	35	50	–	–	–	–	–
Shotcrete	2.4	1250	45	23,875	–	–	–	–	0
Geogrid	0.85	–	–	20	6	0.002	1 × 10 ⁶	2 × 10 ³	20

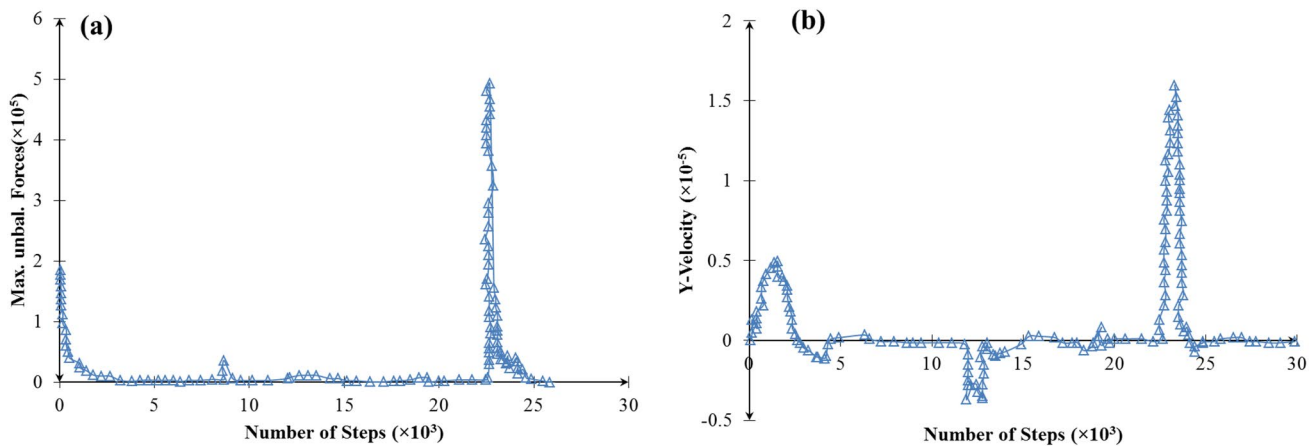


Fig. 9 a Maximum unbalanced forces, b nodal velocity

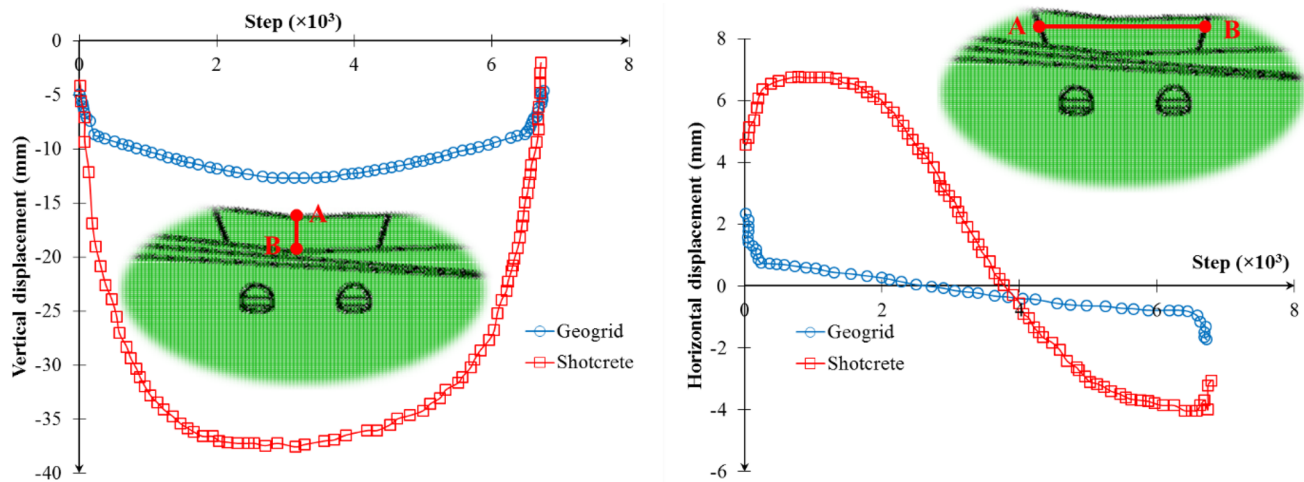


Fig. 10 Vertical and horizontal displacements along the AB line

2.3 mm, while using geogrid. Less deformations occurred in the portal in case of using geogrid rather than shotcrete are due to better performance of geogrid in controlling the plastic zone near to the ground surface. Geogrid restricts the deformations of the host environment by distributing the stresses at a wider range. According to Fig. 10, it can be stated that the geogrid is more capable of controlling the vertical deformations than the horizontal ones.

Geogrid grids restrict the lateral displacements by creating interlocking with soil grains. Also, by changing the stress path, it leads to a change in the failure point and increases soil strength. Even in concentrated loads states, lateral displacement strained by the friction forces and reacts by transferring the activated load as a reaction force back into the soil. The loads imposed on the supporting system in various cases have been presented in Table 4. The results show that after the subsidence of the portal, in spite of the reduction of the overburden, the axial load has been increased. Such a process results from the development of a plastic zone and reaching the failure zone to the ground surface as shown in Fig. 11. According to studies, in shallow tunnels located in soft rocks, only a part of the overburden load is exerted into the supporting system, and the rest is controlled by confining stresses. If the tunnel overburden decreases more than the specified range, the failure zone will reach the ground surface and instead of the plastic zone, the total overburden height will be loaded into the tunnel [34, 35]. No stress relaxation occurs in this case and this results in the design of a heavy supporting system. According to Lei et al. [36], the occurrence of failure in shallow twin tunnels with small clear distance can be summarized as follows: (i) tunnel and strata deformations (ii) deformation propagating to ground surface to lead to subsidence groove and micro-fracture surfaces in the periphery

of tunnel (iii) fracture surfaces extending deep into the surrounding rock in a larger density (iv) tensile cracking in shallow position on deep buried side and shear slip in deep layer (v) rapid deformation and slip on shallow-buried side (vi) collapse.

The moment-axial thrust capacity diagram for initial support (Fig. 12), shows that the supporting system is able to control the loads exerted on it. The method described by Sauer et al. [37] has been used to estimate the moment-axial thrust combinations for the initial support systems.

According to Fig. 13, the plot of forces on the tunnel periphery shows that the application of the geogrid will mainly reduce the axial load and will not have much effect on the bending moment and shear force. By using the geogrid, the axial load exerted on the supporting system would be 43 tons less than the case in which the shotcrete is used. Due to the higher displacements in the left wall of the tunnel, it is realized that monitoring of this section will be of particular importance.

Due to the shallow depth of the tunnel the axial forces, bending moment and shear forces carried by the initial support system are low. The bending moments in the connections between the inverts and the walls (elements 22, 23, 45) are maximum. This is a well-recognized problem in tunnel design and these connections require special designs [38]. The top heading is excavated with “elephant feet” in order to ensure that sufficient capacity is available for the footings of the arch. These elephant feet have to be designed to ensure that there is sufficient reinforcement present to ensure an enough connection between the walls and the invert.

Table 4 The forces exerted on the supporting system in different cases

Element	Before portal collapse			After portal collapse			After using geogrid			After using shotcrete		
	Shear (kN)	Axial (kN)	Mom (kN/m)	Shear (kN)	Axial (kN)	Mom (kN/m)	Shear (kN)	Axial (kN)	Mom (kN/m)	Shear (kN)	Axial (kN)	Mom (kN/m)
22	25.7	148.1	24	25.8	705.6	24.1	20	2.1	18	22.5	31.2	21
21	34.5	491.5	24	42.1	169	24.1	18	556	20.2	26.3	580	21
20	5.3	532.8	3.95	12.2	64.1	10.1	0.05	670	1.3	0.1	713	4.9
19	1.63	572.4	1.28	6.57	296.7	4.1	3	768	3	3.2	826	3.2
18	3.5	613.1	1.6	3.25	666	4.1	1	1013	3.1	1.1	1081	4
17	4.4	668.9	4.04	10.3	856.5	4.12	9.2	1075	1.1	11.4	1148	2.1
16	11.9	723.8	6.28	11.1	937.6	13.7	10.2	1050	11	11.4	1122	12
15	9.04	751.2	6.3	11.8	996.6	13.7	12.1	942	11	13.8	1095	12
14	1.56	823.8	2.85	0.98	1076	3.47	0.3	978	0.3	0.7	1112	0.6
13	7.7	481.7	3.56	11.9	1040	12.6	8.1	950	8.1	9.4	1046	8.4
12	2.4	787.8	3.56	4.85	925	12.5	3.1	910	8.1	3.8	970	8.6
11	5.3	805.5	4.5	5.8	889	10.2	8.2	923	9.1	9.1	1039	10.5
10	11.2	816.6	4.89	6.1	1069	10.2	8.4	875	9	10.5	1307	10.5
9	12.5	770.1	6.46	11.9	920.1	5.7	1.6	987	1.8	5.1	1305	3
8	12.9	761.4	6.4	7.01	727.7	12	10.3	994	13.6	11.9	1239	13.8
7	11.5	653.7	5.2	0.3	562	12	6	1052	13.6	7	1209	13.8
6	5.6	615.1	4.3	4.3	67.2	11.7	0.7	794	3.9	0.8	805	7.9
5	0.03	562.1	0.4	0.6	91.7	8.5	1.23	690	6.6	1.58	712	7.3
4	3.03	495	1.97	9.79	281	8.5	11.2	542	5.5	11.7	558	6.3
3	2.49	416.8	1.97	27.1	265.5	16.5	23.3	561	17	23.2	578	17.8
2	9.6	372.4	6.6	21	449	16.5	16.6	320	16.2	17.2	367	17.8
1	9.1	291	6.5	4.1	457	2.95	7.2	270	6	9.2	297	6.6
<i>Right tube</i>												
45	20.8	327	11.4	41.5	301	22.8	41.2	318.3	20.1	43.5	423	23.8
44	31.8	435	11.4	64.8	107	22.8	58	572.1	22	60.5	673.4	23.8
43	10.7	485	6.05	16.4	207	12.9	12.1	536.8	9	14.7	616	9.3
42	0.6	584	2.97	2.29	102.4	1.06	1	679.2	2.84	1.23	732	3
41	1.46	633.8	3.47	8.02	47.4	4.5	6.1	736.1	6.1	6.9	767	6.6
40	6.98	681.4	3.47	19.6	253.6	11.3	19.4	1014	8.4	19.8	1028	9.3
39	0.95	786.1	2.93	6.67	403.2	16.7	9.4	1002	17.2	10.2	1096	17.6
38	11.2	832	7.05	18.6	572.4	16.7	20.1	975	17.2	21.8	1163	17.6
37	9.08	835.7	7.05	3.2	760.8	3.07	4.2	1102	2.8	5.5	1251	3.2
36	3.8	891.4	0.98	9.5	884.3	4.84	6.2	1123	2.1	7.8	1267	3.3
35	3.7	889.7	2.16	2.17	996.5	6.65	1.7	1251	5	2.7	1268	5.6
34	0.03	839	2.2	1.8	974.1	9.3	0.1	1097	4.12	0.2	1142	5.9
33	3.5	883.5	2.2	8	1137	9.3	4.5	1165	5.5	5.3	1237	5.9
32	0.76	879.2	1.39	4.8	1209	6.6	1.47	1210	2.9	2.3	1302	3.5
31	9.1	817.3	6.67	5.3	1172	11.3	5.6	1181	7.9	5.7	1287	8.6
30	10.7	796.7	6.6	3.57	1138	11.3	1.4	1184	7.9	2.2	1300	8.6
29	0.4	747.9	2.8	4.8	1079	8.1	6	1215	5.3	5.4	1339	6.6
28	7.6	647.7	3.56	8.03	874.7	4.2	5.1	1117	2	5.7	1245	2.4
27	1.46	604.8	3.55	0.7	613.6	2.67	0.8	943	2.12	0.6	1070	2.8
26	1	559	3.36	14.4	439.5	13.3	15.3	873	14.1	15.4	994	14.2
25	12.2	466.3	7.03	17.1	107	1.33	19	654	13.9	20.7	764	14.2
24	36.4	425.4	13	50	329.7	28.7	41	646	26.7	43.4	741	27.2
23	23.7	305.6	13	52.1	400.6	28.7	48.5	268	26.7	49.4	350	27.2

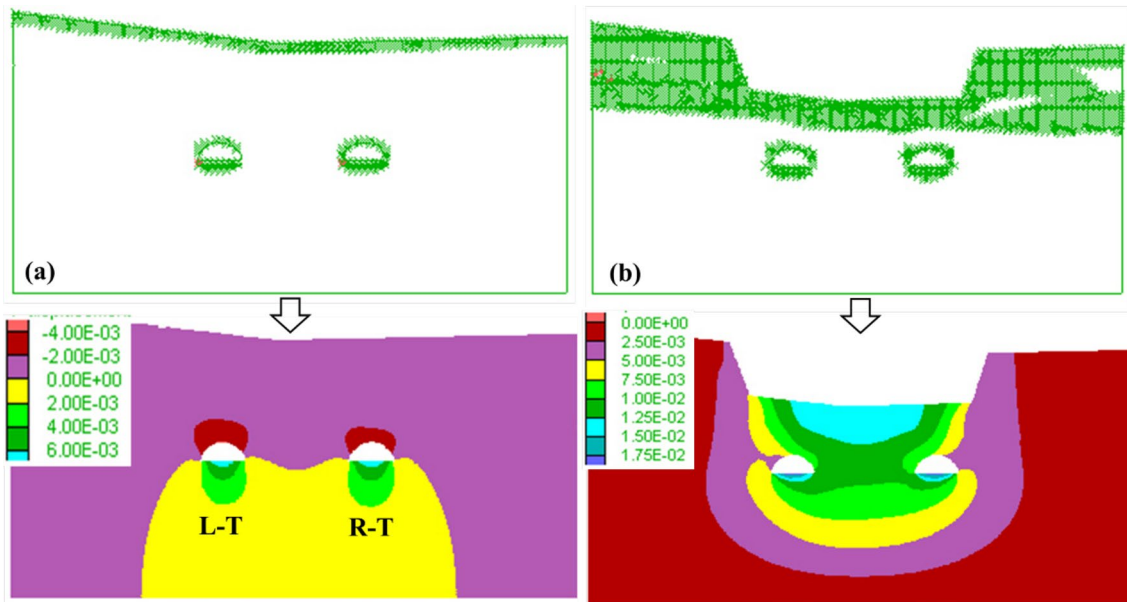


Fig. 11 Status of the plastic zone and rock mass displacements **a** before the collapse, **b** after the collapse

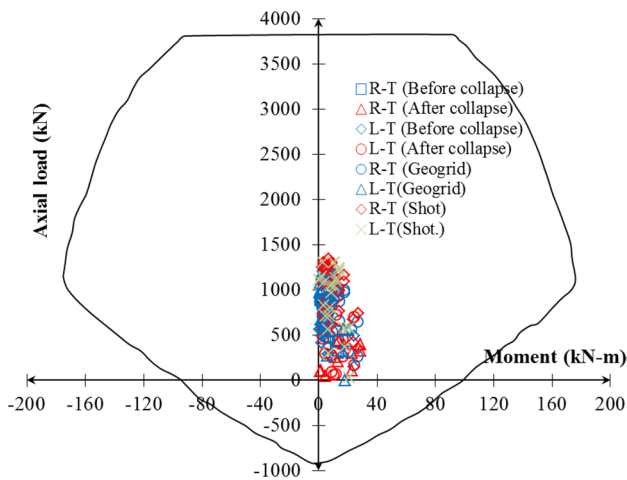


Fig. 12 Moment-axial thrust capacity in different scenarios

Conclusions

In order to rehabilitate the karstic failure of the Heybat Sultan tunnels portal, two methods; shotcreting and soil reinforced with geogrid were investigated. The numerical analyses led to the following results:

- In case of using the geogrid, the amount of portal displacements would be 2.9 times less than that of the shotcrete.

- Geogrid distributes forces at a wider range. Such a function, coupled with its light weight, will bring fewer loads into the tunnel supporting system.
- Geogrid is more capable of controlling the vertical deformations rather than horizontal ones. The vertical and horizontal deformations are observed in the center and sides of the geogrid sheet respectively.
- Geogrid mainly reduces the axial force and has little impact on the bending moment and shear force.
- In shallow tunnels located in soft rocks, due to the absence of stress relaxation, the entire overburden load is transferred to the supporting system. In this case, the use of the elephant feet technique plays a fundamental role in tunnel stability in order to control deformations.

In general, in this case study, based on above reasons, shotcreting is not technically feasible due to the high volume of collapse (2250 m³). Economically, the shotcrete has the highest cost amongst the items in the bill of quantity of Iraqi-Kurdistan projects (200 \$/m³), which is much higher than the alternative of using soil reinforced with geogrid costs.

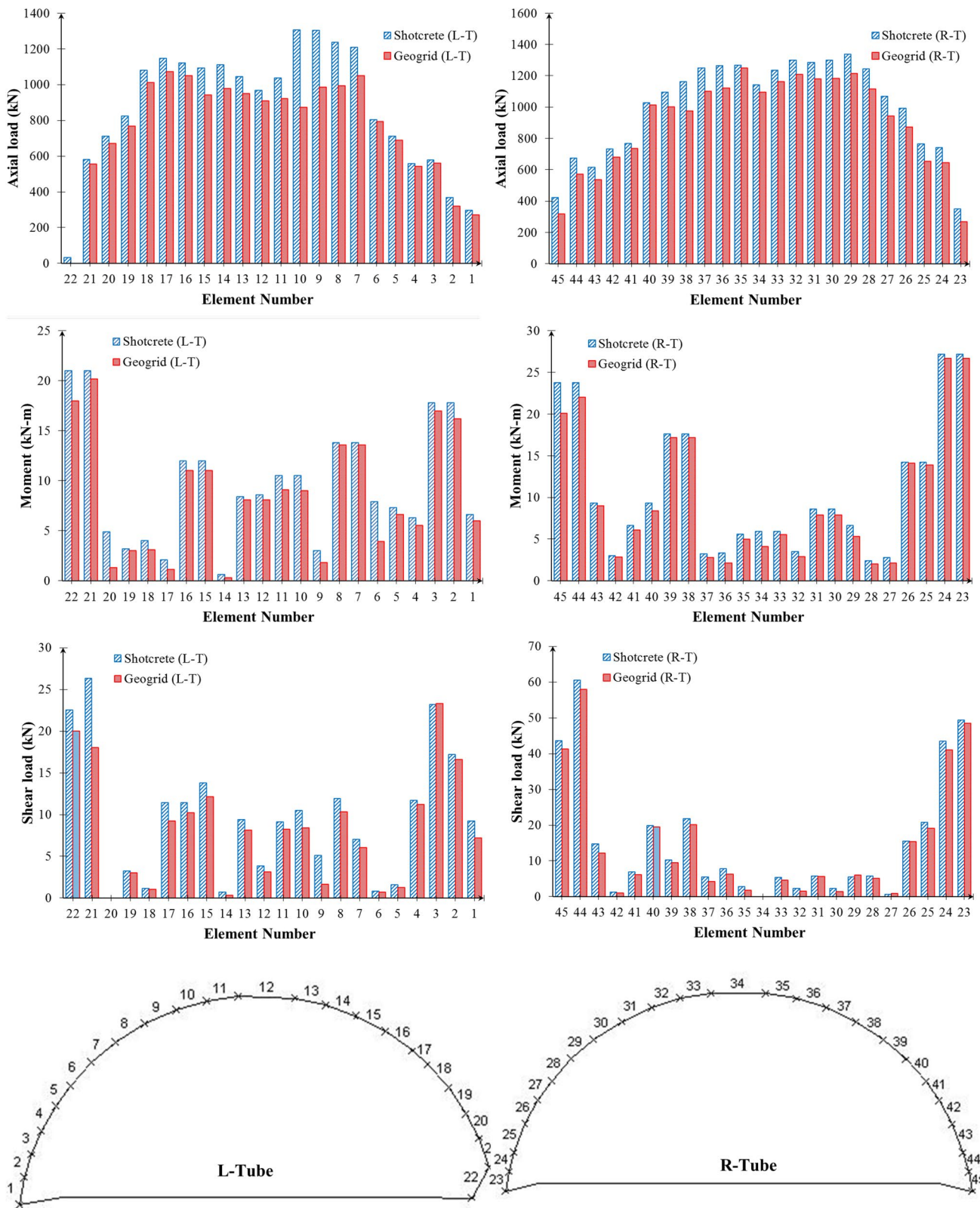


Fig. 13 Forces exerted on the supporting system under different situations

References

- Gutiérrez F, Cooper AH, Johnson KS (2008) Identification, prediction and mitigation of sinkhole hazards in evaporite karst areas. *Environ Geol* 53:1007–1022. <https://doi.org/10.1007/s00254-007-0728-4>
- Li L, Tu W, Shi S, Chen J, Zhang Y (2016) Mechanism of water inrush in tunnel construction in karst area. *Geomat Nat Hazards Risk* 7(Suppl 1):35–46. <https://doi.org/10.1080/19475705.2016.1181342>
- Cui QL, Wu HN, Shen SL, Xu YS, Ye G (2015) Chinese karst geology and measures to prevent geohazards during shield tunnelling in karst region with caves. *Nat Hazards* 77(1):129–152. <https://doi.org/10.1007/s11069-014-1585-6>
- Alija S, Torrijo FJ, Quinta-Ferreira M (2013) Geological engineering problems associated with tunnel construction in karst rock masses: the case of Gavarres tunnel (Spain). *Eng Geol* 157:103–111. <https://doi.org/10.1016/j.enggeo.2013.02.010>
- Song K, Cho G, Chang S (2012) Identification, remediation, and analysis of karst sinkholes in the longest railroad tunnel in South Korea. *Eng Geol* 135–136:92–105. <https://doi.org/10.1016/j.enggeo.2012.02.018>
- Li S, Zhou Z, Li L, Xu Z, Zhang Q, Shi S (2013) Risk assessment of water inrush in karst tunnels based on attribute synthetic evaluation system. *Tunn Undergr Space Technol* 38:50–58. <https://doi.org/10.1016/j.tust.2013.05.001>
- Huang F, Zhaob L, Linga T, Yang X (2017) Rock mass collapse mechanism of concealed karst cave beneath deep tunnel. *Int J Rock Mech Min Sci* 91:133–138. <https://doi.org/10.1016/j.ijrmm.2016.11.017>
- Elleboudy AM, Saleh NM, Salama AG (2017) Assessment of geogrids in gravel roads under cyclic loading. *Alex Eng J* 56:319–326. <https://doi.org/10.1016/j.aej.2016.09.023>
- Hussein MG, Meguid MA (2016) A three-dimensional finite element approach for modeling biaxial geogrid with application to geogrid-reinforced soils. *Geotext Geomembr* 44:295–307. <https://doi.org/10.1016/j.geotextmem.2015.12.004>
- Ziegler M (2017) Application of geogrid reinforced constructions: history, recent and future developments. *Procedia Eng* 172:42–51. <https://doi.org/10.1016/j.proeng.2017.02.015>
- Kayadelen C, Önal T, Altay G (2018) Experimental study for pull-out load of reinforced sand soil with geogrid. *Measurement* 117:390–396. <https://doi.org/10.1016/j.measurement.2017.12.024>
- Mekonnen AW, Mandal JN (2017) Behavior of bamboo-geogrid reinforced fly ash wall under applied strip load. *Int J Geosynth Ground Eng* 3:24. <https://doi.org/10.1007/s40891-017-0105-7>
- Yu Y, Bathurst RJ, Allen TM, Nelson R (2016) Physical and numerical modelling of a geogrid reinforced incremental concrete panel retaining wall. *Can Geotech J* 53(12):1883–1901. <https://doi.org/10.1139/cgj-2016-0207>
- Biswas A, Ansari MDA, Dash SK, Krishna AM (2015) Behavior of geogrid reinforced foundation systems supported on clay subgrades of different strength. *Int J Geosynth Ground Eng* 1:20. <https://doi.org/10.1007/s40891-015-0023-5>
- Allen TM, Bathurst RJ (2014) Performance of an 11 m high block-faced geogrid wall designed using the K-stiffness method. *Can Geotech J* 51(1):16–29. <https://doi.org/10.1139/cgj-2013-0261>
- Shukla SK (2002) *Geosynthetics and their applications*. Thomas Telford Publishing, London
- Shukla SK, Yin JH (2006) *Fundamentals of geosynthetic engineering*. Taylor and Francis, London
- Shukla SK (2012) *Handbook of geosynthetic engineering*, 2nd edn. ICE Publishing, London
- Xiao C, Han J, Zhang Z (2016) Experimental study on performance of geosynthetic-reinforced soil model walls on rigid foundations subjected to static footing loading. *Geotext Geomembr* 44(1):81–94. <https://doi.org/10.1016/j.geotextmem.2015.06.001>
- Bathurst RJ (1990) Instrumentation of geogrid-reinforced soil walls. *Transp Res Rec* 1277:102–111
- Bathurst RJ, Benjamin DJ, Jarrett PM (1988) Laboratory study of geogrid reinforced soils walls. ASCE special publication no. 18, geosynthetics for soil improvement, pp 178–192
- Liu C, Yang K, Ho Y, Chang C (2012) Lessons learned from three failures on a high steep geogrid-reinforced slope. *Geotext Geomembr* 34:131–143. <https://doi.org/10.1016/j.geotextmem.2012.05.003>
- Ali HF (1993) Field behaviour of a geogrid-reinforced slope. *Geotext Geomembr* 12(1):53–72. [https://doi.org/10.1016/0266-1144\(93\)90036-N](https://doi.org/10.1016/0266-1144(93)90036-N)
- Daraei A, Herki BMA, Sherwani AFH, Zare S (2018) Slope stability in swelling soils using cement grout: a case study. *Int J Geosynth Ground Eng* 4:10. <https://doi.org/10.1007/s40891-018-0127-9>
- Reif D, Decker K, Grasemann B, Peresson H (2012) Fracture patterns in the Zagros fold-and-thrust belt, Kurdistan Region of Iraq. *Tectonophysics* 576–577:46–62. <https://doi.org/10.1016/j.tecto.2012.07.024>
- Frehner M, Reif D, Grasemann B (2012) Mechanical versus kinematical shortening reconstructions of the Zagros High Folded Zone (Kurdistan region of Iraq). *Tectonics* 31:TC3002. <https://doi.org/10.1029/2011TC003010>
- Beiniawski ZT (1989) *Engineering rock mass classifications*. Wiley, New York
- Daraei R, Herki BMA, Sherwani AFH (2017) Study on the rapid drawdown and its effect on portal subsidence of Heybat Sultan twin tunnels in Kurdistan-Iraq. *Civ Eng J* 3(7):496–507
- Daraei A, Zare S (2018) Effect of water content variations on critical and failure strains of rock. *KSCE J Civ Eng*. <https://doi.org/10.1007/s12205-018-0592-7>
- Choudhary AK, Krishna AM (2016) Experimental investigation of interface behaviour of different types of granular soil/geosynthetics. *Int J Geosynth Ground Eng* 2:4. <https://doi.org/10.1007/s40891-016-0044-8>
- Itasca Consulting Group Inc (2002) *Fast lagrangian analysis continua. FLAC Ver. 4.0 user manuals*
- Hoek E, Carranza-Torres C, Diederichs MS, Corkum B (2008) Integration of geotechnical and structural design in tunnelling. In: *Proceedings University of Minnesota 56th Annual Geotechnical Engineering Conference*, Minneapolis, pp 1–53
- Tong J, Karakus M, Wang M, Dong C, Tang X. (2016) Shear strength characteristics of shotcrete-rock interface for a tunnel driven high rock temperature environment. *Geomech Geophys Geo-energy Geo-resour* 2:331–341. <https://doi.org/10.1007/s40948-016-0039-x>
- Hoek E (2004) Numerical modelling for shallow tunnels in weak rock. Discussion paper # 3. <http://www.rocsience.com>
- Mishra S, Rao KS, Gupta NK, Kumar A (2017) Damage to shallow tunnels under static and dynamic loading. *Procedia Eng* 173:1322–1329. <https://doi.org/10.1016/j.proeng.2016.12.171>
- Lei M, Lin D, Yang W, Shi C, Peng L, Huang J (2016) Model test to investigate failure mechanism and loading characteristics of shallow-bias tunnels with small clear distance. *J Cent South Univ* 23:3312–3321. <https://doi.org/10.1007/s11771-016-3397-1>
- Sauer G, Gall V, Bauer E, Dietmaier P (1994) Design of tunnel concrete linings using limit capacity curves. In: *Siriwardane, Zaman (eds) Computer methods and advances in geomechanics*. Balkema, Rotterdam, pp 2621–2626
- Hoek E (2003) Integration of geotechnical and structural design in weak rock tunnels. <http://www.rocsience.com>